iScience

Article

Hyperglycemic milieu impairs Vγ9Vδ2 T cell functions in tuberculosis patients and prolongs M.tb negative conversion time

Graphical abstract

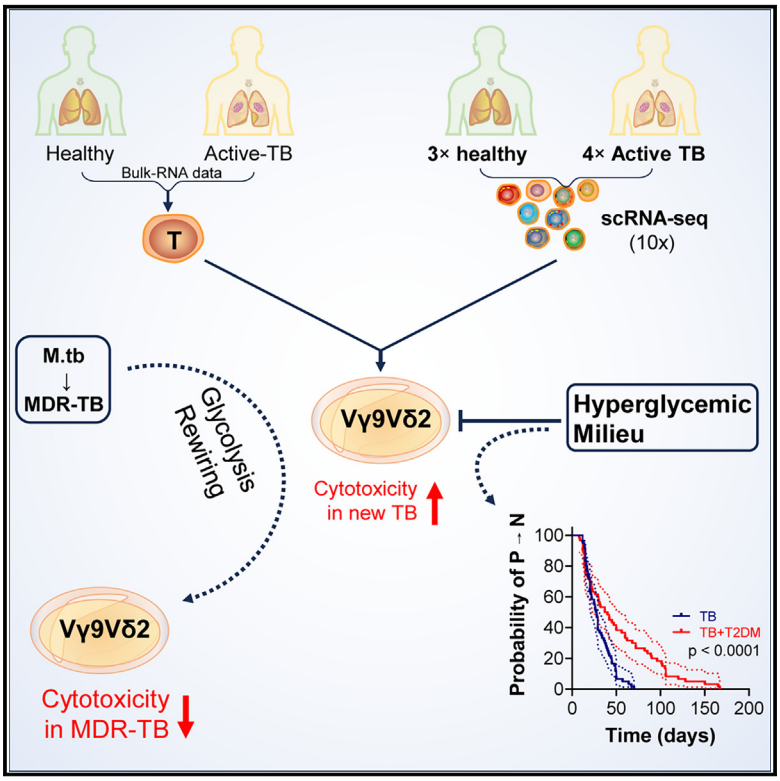

Highlights

- Reduced Vδ2⁺CD3 T cells mark peripheral γδ T cell imbalance in TB patients
- Glucose metabolism dysregulation impairs γδ T cells' anti-infection function in TB
- Excessive glucose suppresses the CD107a expression of Vδ2⁺γδ T cells
- Hyperglycemia links to γδ T cell dysfunction, MDR-TB emergence, and poor prognosis

Authors

Meiyan Li, Jing Liu, Yanyun Jing, ..., Yi Cai, Yangzhe Wu, Yi Hu

Correspondence

caiyi0113@szu.edu.cn (Y.C.),
tyzwu@jnu.edu.cn (Y.W.),
yihu2020@jnu.edu.cn (Y.H.)

In brief

Immunology; Microbiology

Li et al., 2025, iScience *28*, 111692
January 17, 2025 © 2024 The Authors. Published by Elsevier Inc.
https://doi.org/10.1016/j.isci.2024.111692

CellPress

iScience

CellPress
OPEN ACCESS

Article

Hyperglycemic milieu impairs Vγ9Vδ2 T cell functions in tuberculosis patients and prolongs M.tb negative conversion time

Meiyan Li,[1,6] Jing Liu,[2,3,6] Yanyun Jing,[3,6] Yanqin Song,[1,6] Xuezhi Wang,[1,6] Qinglin Hu,[2,3] Minjing Hong,[3] Yijia Li,[3] Chan Xiong,[3] Yi Cai,[4,*] Yangzhe Wu,[3,*] and Yi Hu[2,5,7,*]

[1]Department for Tuberculosis, The Fourth People's Hospital of Foshan, Foshan 528000, Guangdong, China
[2]Microbiology and Immunology Department, School of Medicine, Faculty of Medical Science, Jinan University, Guangzhou 510632, Guangdong, China
[3]Guangdong Provincial Key Laboratory of Tumour Interventional Diagnosis and Treatment, Zhuhai Institute of Translational Medicine, Zhuhai People's Hospital (The Affiliated Hospital of Beijing Institute of Technology, Zhuhai Clinical Medical College of Jinan University), Zhuhai 519000, Guangdong, China
[4]Guangdong Provincial Key Laboratory of Infection Immunity and Inflammation, Department of Pathogen Biology, Shenzhen University Medical School, Shenzhen, China
[5]Key Laboratory of Viral Pathogenesis & Infection Prevention and Control (Ministry of Education), Jinan University, Guangzhou 510632, China
[6]These authors contributed equally
[7]Lead contact
*Correspondence: caiyi0113@szu.edu.cn (Y.C.), tyzwu@jnu.edu.cn (Y.W.), yihu2020@jnu.edu.cn (Y.H.)
https://doi.org/10.1016/j.isci.2024.111692

SUMMARY

γδ T cells play protective roles in tuberculosis (TB). Our work demonstrated the therapeutic potential of allogeneic Vγ9Vδ2 T cells in TB patients. However, their functions in TB require further comprehensive evaluation. Here, we compared γδ T cells in TB patients and healthy adults at the bulk and single-cell RNA and protein levels, revealing that impaired glucose metabolism critically undermines their anti-infective functions. Excessive glucose disrupts γδ T cell effector functions, correlating with prolonged sputum smear conversion time in TB patients with type II diabetes. Additionally, serum glucose levels were linked to multidrug-resistant TB. These findings suggest that weakened Vδ2$^+$γδ T cell responses in diabetic TB patients contribute to multidrug resistance. Restoring Vδ2$^+$γδ T cell function offers a promising strategy for TB treatment.

INTRODUCTION

Tuberculosis (TB), caused by Mycobacterium tuberculosis (*M.tb*), is a highly contagious disease. While a quarter of the world's population is estimated to have been infected, most can clear the infection. However, TB disease can be deadly without proper treatment.[1] Moreover, the emergence of multidrug-resistant TB, known as MDR-TB, poses a significant challenge.[2] Understanding the disease mechanism is crucial to achieve the goal of ending the global TB epidemic.

Immune functions of γδ T cells in TB

TB progression is influenced by *M.tb*'s evasion of the host immune system.[3] γδ T cells play a crucial role in the immune responses to TB, making them a potential target for TB vaccine development.[4] Furthermore, our groundbreaking clinical application of allogeneic Vδ2$^+$γδ T cell therapy in MDR-TB treatment further highlighted the protective role of γδ T cells in TB.[5]

In humans, γδ T cells make up 1–5% of the T cell population in peripheral blood but are enriched in the intestine and skin.[6] γδ T cells are a distinct subset of lymphoid cells that possess characteristics of both innate and adaptive immunity.[7] Notably, γδ T cells can function as professional antigen-presenting cells (APCs)[8] and regulate various components of the immune system, including αβ T cells,[9] B cells,[10] dendritic cells,[11,12] and macrophages.[13] Moreover, γδ T cells uniquely recognize antigens independently of major histocompatibility complex (MHC) molecules.[14,15] This unique feature enables them to perform nonredundant functions compared to αβ T cells, ensuring broader protection against pathogens.[16]

Three major γδ T cell subsets, namely Vδ1$^+$, Vδ2$^+$, and Vδ3$^+$, can be detected in humans. The Vδ2$^+$ subset predominantly pairs with Vγ9 TCR and constitutes the main γδ T cell population in circulating blood, known as Vγ9Vδ2 T cells. On the other hand, Vδ1$^+$ cells are mainly found in tissues such as the gut epithelium, skin, etc. Furthermore, Vγ9Vδ2 T (namely Vδ2 onward) cells play a role in innate immune responses, while Vδ1$^+$ γδ T cells exhibit characteristics of adaptive immune cells.[17,18] Specifically, unlike other γδ T subsets, Vδ2$^+$ TCRs recognize phosphoantigens (pAgs) produced by *M.tb* and other pathogens,[4] indicating non-redundant roles of specific γδ T cell subsets in mediating immune responses.[18] Since Vδ1$^+$ and Vδ2$^+$ are the two predominant subsets in peripheral blood, we will limit our exploration on these two in this study.

This is an open access article under the CC BY-NC license (http://creativecommons.org/licenses/by-nc/4.0/).

Hyperglycemia, diabetes, and tuberculosis

Hyperglycemia, characterized by high blood sugar levels, strongly associates with TB. It is considered a risk factor for TB infection and poor outcomes in TB patients.[19] Hyperglycemia is commonly seen in individuals with diabetes, and poorly controlled blood glucose levels can have detrimental effects on the immune system.[20] Studies have shown that individuals with diabetes have an increased susceptibility to TB, as hyperglycemia impairs the immune system's ability to respond effectively to the infection. Diabetes not only raises the risk of developing active TB and reactivating latent TB but also contributes to the emergence of drug-resistant TB.[21] Recent studies have demonstrated increased likelihood of treatment failure in TB patients with diabetes.[22] High glucose levels have been linked to the development of autoimmune diseases.[23] Additionally, metabolic abnormalities in diabetes have been shown to weaken the effector functions of γδ T cells.[24]

To investigate the impact of glucose levels on immune functions, we performed immune phenotyping on TB patients with normal or elevated fasting serum glucose levels. We observed compromised anti-TB infection function of γδ T cells in both groups. At the molecular level, we found enrichment of glycolytic and diabetes-related pathways in γδ T cells of TB patients. Clinical sample examination confirmed that MDR-TB patients had higher glucose levels, elevated immunosuppressive marker C-reactive protein (CRP), and impaired γδ T cell effector function. Furthermore, our analysis of sputum conversion time in TB patients revealed that hyperglycemia negatively affected the outcome of TB treatment. These findings indicate that hyperglycemia compromises the effector function of Vδ2$^+$ T cells, increasing the risk of TB progressing to MDR-TB.

RESULTS

Bulk RNA-seq suggests compromised immune cell functions in active TB patients

The analysis of the bulk RNA-seq dataset (GSE19444) from peripheral blood mononuclear cells (PBMCs) of individuals with latent TB compared to healthy donors revealed minimal impact at the RNA level, indicating by only 143 upregulated genes and 85 downregulated genes (Figure S1A). However, comparing to individuals with latent TB, individuals with active TB (GSE37250) showed significant variations in gene expressions, evidenced by 2952 upregulated genes and 3811 downregulated genes (Figure 1A). Gene Ontology (GO) and Kyoto Encyclopedia of Genes and Genomes (KEGG) enrichment analyses identified top 20 upregulated and downregulated pathways associated with T cell functions. For example, innate immune responses including the NOD-like receptor signaling pathway were upregulated, while T cell receptor signaling pathway and pathways related to DNA, RNA, and protein synthesis were downregulated in active TB patients (Figure S1B). These results show the overall difference in the immune landscape of PBMCs between the inflamed (active TB) and the quiescent state (latent TB). Furthermore, we focus on analyses of key genes related with T cell recognition/activation (Figure 1C), checkpoint (Figure 1B) and effector (Figure 1D). It shows that recognition/activation-related genes such as *CD3D/E*, *CD4*, *CD8A/B*, *CD28*, and *ICOS*, and protease-related genes such as *GZMK* and *GZMB* were downregulated. Whereas genes of inhibitory checkpoints appear to be inconsistent, including significant upregulations of *PDL1, HAVCR2*, and *CD39*, and downregulations of *CTLA4*, *CD73*, *PDCD1*, and *TIGIT*. These phenotypes collectively suggest impaired immune responses of peripheral immune cells in active TB patients.

To compensate the limitations of bulk-RNA sequencing in analyzing cell-type-specific gene expression, we then employed flow cytometry analysis to investigate the functions of two major cytotoxic subsets of T cells in active TB patients, γδ T cells and CD8$^+$ T cells. Results indicate a significant downregulation of Vδ2$^+$, while Vδ1$^+$ T cell population remained relatively unchanged, resulting an inversion of the Vδ1/Vδ2 ratio in TB patients, while the percentage of CD8$^+$ T cells remained unaltered (Figures 2A and 2B). Notably, the phenotype of inverted Vδ1/Vδ2 ratio have been also observed in our previous reports,[25,26] which is likely associated with the impaired immune responses in infectious and cancerous diseases [49, 50], appearing to be a common phenotype in population with diseases. Furthermore, analyses indicated that cytokines and effector molecules essential for recognition and infection clearance, including NKG2D, IFNγ, and TNFα were significantly downregulated (Figure 2C). Interestingly, molecules responsible for T cell activation and degranulation upon stimulation, CD226 and CD107a, respectively, showed a significant increase (Figure 2D). Additionally, the protein expression levels of IL17 and TGFβ were also increased, suggesting the presence of an inflammatory responses of Vδ2 T cells induced by TB infection (Figure 2E). We also assessed the expression of key immune checkpoint molecules on Vδ2$^+$ cells of TB patients and observed a downregulation of CD73, but no significant changes in LAG3 and PD1 molecules (Figure 2F). Similar immune profiles were also observed in CD8$^+$ T cell subset (Figures S2A and S2B), which consistently exhibit elevated IL17, TGFβ, CD226, and CD107a, but reduced IFNγ and TNFα. Overall, these results indicate impaired immune responses of Vδ2 T cells and CD8$^+$ T cells in TB patients, highlighting the significance of the Vδ2 T cell population for further investigation.

scRNA-seq analysis of human γδT cells in PBMCs of TB patients and healthy donors

To investigate the functional characteristics of γδ T cells in TB patients, we performed single-cell RNA sequencing (scRNA-seq) using PBMCs from 4 newly diagnosed TB patients. We compared the scRNA-seq data with publicly available datasets from 3 healthy donors obtained from the official website of 10x Genomics, a schematic overview is depicted (Figure 3A). Our analysis revealed an expansion of T and NK cell populations, accompanied by a decrease in monocyte and B cell populations in active TB patients (Figure 3B). By using signature genes specific to γδ T cells (*CD3* and *TRDC*), we extracted the γδ T cell population for further functional analysis (Figure 3C).

γδ T cell clustering and subtype analyses

We identified six unique γδ T cell clusters based on their gene expression profiles (upper panel of Figure 3C). In healthy donors, a relatively similar distribution of clusters was observed across

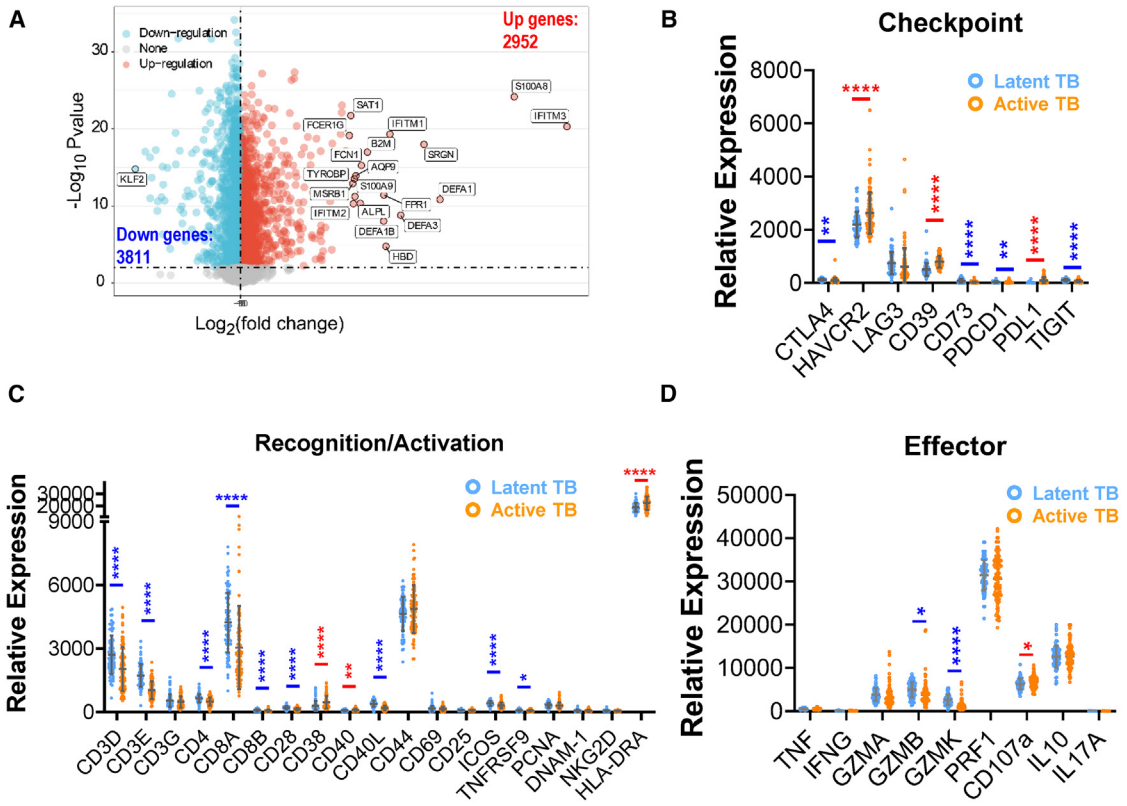

Figure 1. Bulk RNA analyses performed on active and latent TB patients using GEO database

(A) Volcano-map showing upregulated (red, total of 2962 genes) and downregulated genes (blue, total of 3811 genes).

(B) Checkpoint molecules expression of latent and active TB patients.

(C) Recognition and activation related gene expression of latent and active TB patients.

(D) Gene expression of key effector molecules of latent and active TB patients. Active TB patients: $n = 97$; latent TB patients: $n = 83$. Quantitative data are shown as the mean ± SD. *$p < 0.05$, **$p < 0.01$, ***$p < 0.001$, ****$p < 0.0001$; unmarked, not significant. Red *, upregulation; blue *, downregulation. GZM, granzyme; PFN1, perforin-1. Data are represented as mean ± SD.

individuals, indicating a consistent immune status. However, in TB patients, we observed diverse cluster distribution patterns, suggesting a heterogeneous immune response in these individuals (lower panel of Figure 3C). To explore the characteristics of each cluster, we analyzed the top 10 Differentially Expressed Genes (DEGs) in each cluster and visualized them in a heatmap (Figure 3D). Additionally, we selected representative marker genes for demonstration using UMAP plots (Figure 3E). Subsequently, we provide a summary of the key annotation and marker genes for each cluster (Figures 3D, 3E and Table S1). Cluster 1 (C1 - NK-like cytotoxic): This cluster was the most abundant in both TB patients and healthy donors. It expressed genes associated with cytotoxic immune cells, such as *CCL3, GNLY, KLRF1, PRF1,* and *GZMB*. Cluster 2 (C2 - Vγ9Vδ2): This cluster was also highly populated in both healthy and diseased samples. It was characterized by the expression of *TRDV2, TRGV9*, and inhibitory checkpoint molecule like *LAG3*, indicating an inhibitory population of γδ T cells. Cluster 3 (C3 - naive): This cluster exhibited high expression of genes such as *LEF1*, *CCR7*, *TCF7*, and *IL7R*, suggesting a subset of naive γδ T cells. Cluster 4 (C4 - ADCC): This cluster was distinguished by the high expression of the Antibody Dependent Cell Cytotoxicity (ADCC) marker *FCGR3A (CD16)* and recognition or cytotoxicity markers like *KLRC3 (NKG2E)*, *GZMB*, and *GZMH*. Cluster 5 (C5 - XCL$^+$): This minor population showed high expression of chemokine genes involved in mediating dendritic cell functions, such as *XCL1* and *XCL2*. This cluster likely represents a population mediating cell-cell interactions. Cluster 6 (C6 - proliferating): This minor population was detected in both healthy and diseased samples and strongly expressed proliferating cell markers such as *TYMS*, *MKI67*, *CDC45*, *BIRC5*, and *PCNA*. Moreover, we performed comprehensive functional enrichment analysis for each distinct cluster (Figure 3F), employing Gene Set Enrichment Analysis (GSVA). This analysis further underscores the functional diversity inherent within each cluster. Comparing cluster distribution between TB patients and healthy controls showed a decrease in naive, cytotoxic, and proliferating populations, but an increase in the exhausted Vγ9Vδ2 population among TB patients. This suggests impaired anti-infection responses of γδ T cells. These findings provide direct overview of functional and compositional differences in peripheral γδ T cells between healthy individuals and TB patients.

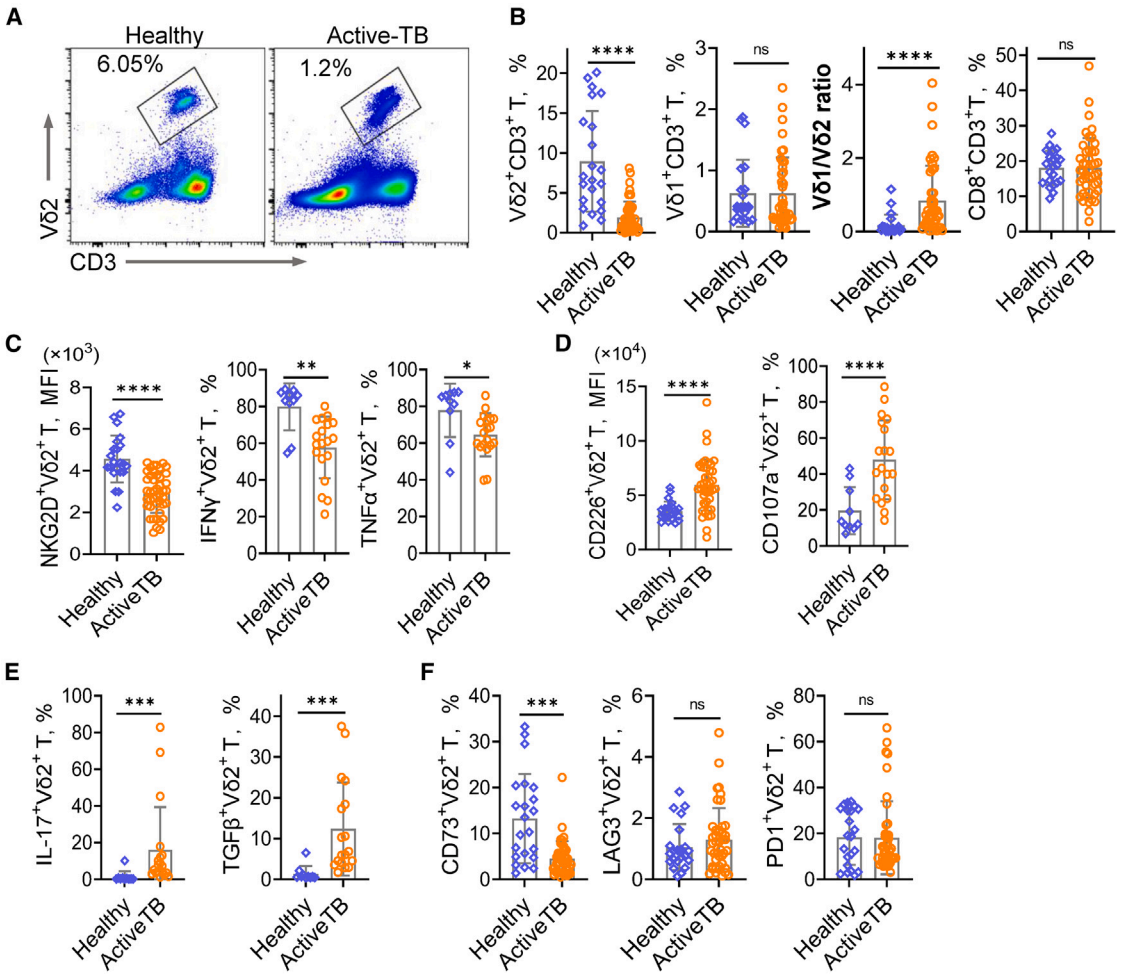

Figure 2. Immune function evaluations on γδ T and CD3 T cells using flow cytometry

The PBMCs samples were collected from peripheral blood of either healthy donors or active TB patients.

(A) Representative flow plots of $Vδ2^+γδ$ T cells. b. Flow cytometry evaluations on $Vδ1^+$, $Vδ2^+$, Vδ1/Vδ2, and $CD8^+$ T cells in active TB patients and healthy donors. (C–F) Flow cytometry evaluations on NKG2D, IFNγ, TNFα, CD226, CD107a, IL-17, TGFβ, CD73, LAG3, and PD1 of Vδ2 T cells in active TB patients and healthy donors. Flow gating of these molecules was performed based on graph (a), and the percentages represent the proportion of Vδ2 T cells that express a specific molecule among total Vδ2 T cells. Active TB patients: $n = 44$; healthy donors: $n = 22$. Quantitative data are shown as the mean ± SD. $^*p < 0.05$, $^{**}p < 0.01$, $^{***}p < 0.001$, $^{****}p < 0.0001$; ns, not significant. Data are represented as mean ± SD.

Developmental trajectory and state transition of γδ T cells

To understand the functional evolution from healthy to TB status, we projected the γδ T cell clusters and sample groups onto a two-dimensional pseudo-time plot to analyze the developmental trajectory of these cells (Figure 4A). It is noteworthy that cluster 6 was excluded from this analysis due to its pronounced proliferative characteristics, which could potentially confound the pseudo-time result. Utilizing Monocle, we generated a branched structure comprising seven distinct cellular states and four gene expression modules. Among these states, we defined state 1, 2, and 7 as the pre-branch (Figure S3A), which represented the starting point of the pseudo-time analysis (Figure 4A). These states exhibited high expression of naive markers such as *LEF1, TCF7, CCR7*, and *IL7R*. States 4–6 and state 3 indicated differentiated effector functional transitions, with state 3 predominantly consisting of cells from TB patients and state 4–6 containing a mixture of cells from both TB patients and healthy individuals. This observation underscores the disparate pseudo-time evolution of γδ T cells between the two cohorts (Figure 4A). Furthermore, gene module analyses and sample distribution patterns across the pseudo-time scale provide insights into functional transitions and differences between healthy and diseased cells (Figure 4B), showing naive cells are dominant in healthy while inhibitory and antigen-presenting cells dominate in TB group.

Specifically, we observed four distinct gene expression modules and identified representative functional genes within each module (Figure 4B). The analysis revealed that healthy γδ T cells mainly distributed in the pre-branch states and exhibited high expression of naive markers, aligning with the higher ratio of naive γδ T cells in healthy controls, as indicated by the gene

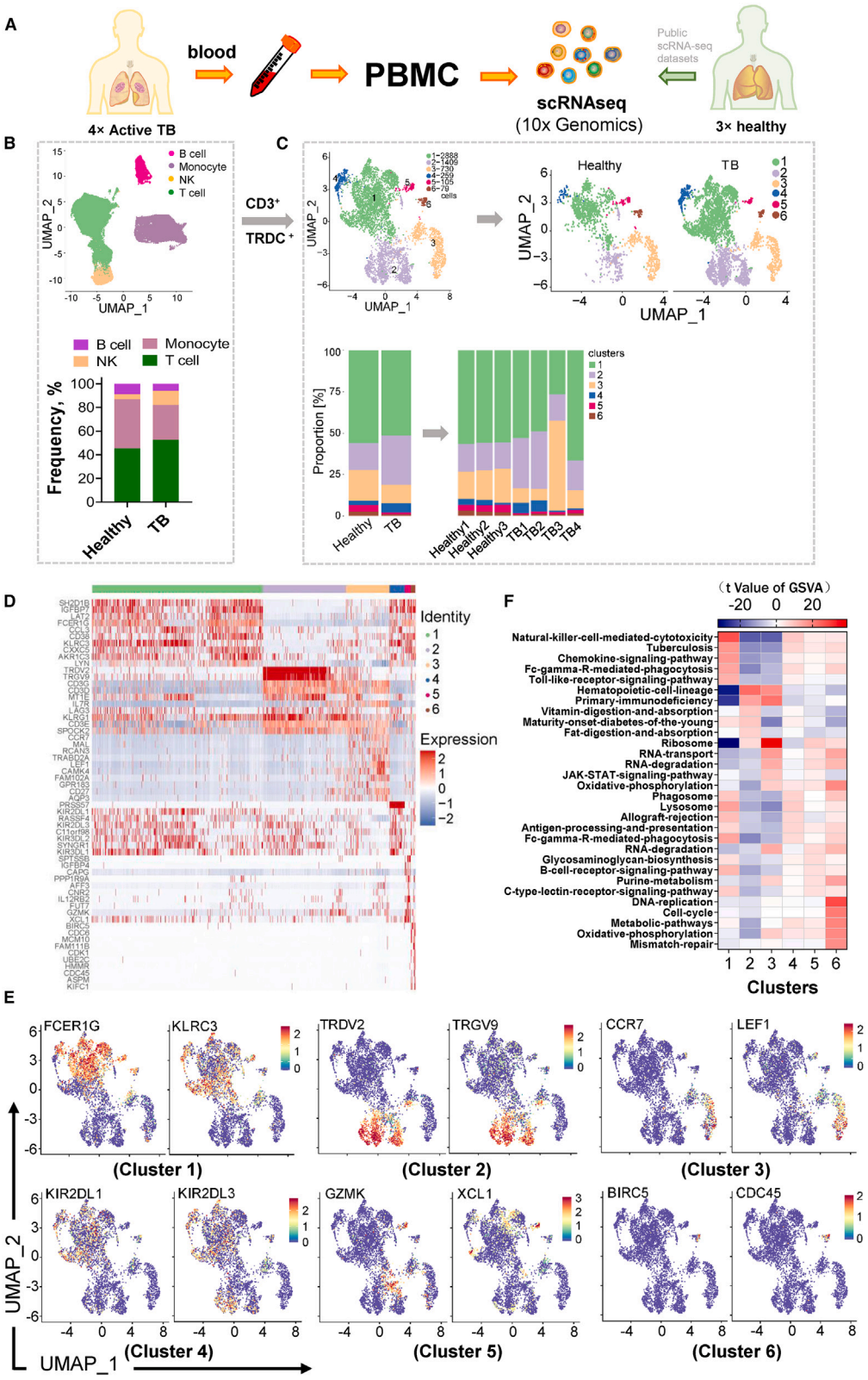

(legend on next page)

expression patterns in module 2. Conversely, cells showing a high expression of genes in module 3 were predominantly derived from TB patients. Further analysis of genes displaying module 3 patterns indicated that γδ T cells from TB patients were activated but exhibited high levels of exhaustion. This was evident from the expression of a group of MHC II genes and immune checkpoint molecules such as *LAG3* and *CTLA4*.

Lastly, module 1 and 4 contained effector and cytokine genes, including *XCL1, XCL2, GZMB, GNLY*, and *PRF1*, which were observed in both TB and healthy cells, representing universal functional effector cell subsets in these two groups. The pseudo-time evolution of key functional genes is depicted in Figure 4C, and further functional enrichments of individual modules can be found in Figure S3B. Therefore, the results in Figure 4 suggest that γδ T cells in TB display distinct functional alterations, characterized by an activated yet exhausted immune phenotype.

γδ T cells show reduced proliferation and cell cycle disruption in TB

Given the notable reduction of the proliferative cluster 6 in TB patients, we proceeded to compare the γδ T cell cycle progression between TB and healthy samples. The GSEA of crucial cell cycle-related terms (G2M checkpoint, mitotic spindle, and cell cycle) revealed significant downregulation in TB samples, suggesting potential cell cycle dysregulation (Figure 5A).

Cell cycle analyses were conducted on the scRNA-seq data to investigate cell cycle phases within clusters and across TB and healthy samples. Intriguingly, clusters 2 and 4, which demonstrated elevated proportions in TB patients (Figure 3C), exhibited a higher percentage of cells in the G1 phase and a lower percentage in the G2M phase compared to the other four clusters (Figure 5B). Moreover, significant disparities were observed in the distribution of the G1, G2M, and S phases between γδ T cells derived from healthy individuals and TB patients (Figure 5C). TB patients demonstrated reduced proportions of cells in the G2M and S phases, along with an elongated G1 phase. This observation corroborates the disruption of cell proliferation, representing an aspect of impaired functionality in γδ T cells during TB infection.

Hyperglycemia correlates with γδ T cell malfunction

To further explore the impact of TB burden on γδ T cell functions, we conducted KEGG pathway enrichment analyses (Figure 6A) using scRNA-seq data and identified significant upregulation of pathways related to glycolysis and type 1 diabetes mellitus in TB patients. In contrast, the TCR signaling pathway was found to be downregulated. These findings are consistent with the bulk RNA-seq data obtained from PBMCs of TB patients and healthy donors, which showed increased RNA expression of key enzymes involved in glycolysis, such as *LDHA, HK2*, and *PKM* (Figure 6B). We then performed Gene set variation analysis (GVSA) to evaluate pathways associated with glucose metabolism (Figure 6C), revealing the upregulation of glucose metabolism-related pathways such as diabetes and glycan biosynthesis of γδ T cells in TB patients. Conversely, B-, T cell receptor signaling, insulin signaling pathways were enriched in healthy samples, suggesting normal adaptive immunity and well-regulated glucose metabolism. The activation of glycolysis-related pathways may be attributed to the excess supply of glucose in the peripheral blood of TB patients.

To further investigate the relationship between serum glucose levels and γδ T cell phenotypes, we performed immune phenotyping on γδ T cells from active TB patients with normal glucose levels (NG) and hyperglycemia (HG) (Figure 6D). Interestingly, comparing with NG TB patients, we observed a further reduction in the Vδ2$^+$ population specifically in TB patients with hyperglycemia (both NG and HG populations have significant lower Vδ2 percentage comparing to healthy population, see Figure 2B), while no significant changes were observed in the Vδ1$^+$ and CD8$^+$ T cells. Furthermore, the expression level of CD226, an activation marker, was also reduced in Vδ2$^+$ T cells from TB patients with hyperglycemia, but no statistical difference observed for expressions of PD-1, LAG-3, IFNγ, TNFα, and CD107a (Figures 6E and S4A). Based on clinical data, we further conducted a correlation analysis and found a negative correlation between serum glucose levels and CD226 expression, suggesting that excessive glucose may impair the activation of Vδ2$^+$ T cells. Meanwhile, there is a positive correlation between serum glucose levels and expressions of PD-1 and LAG-3, suggesting a possible link between hyperglycemia and immunosuppression (Figure 6F).

Given the established association of diabetes and hyperglycemia with heightened TB susceptibility, we hypothesize that high glucose level in TB patient is one of key factors in compromising Vδ2 T cell effector functions against TB infections. Notably, similar observation of impaired γδ T cell-mediated anti-tumor function has been reported on cancer patients with diabetes.[24] To investigate the impact of high glucose levels on γδ T cell effector functions, we conducted *in vitro* experiments using Vδ2 T cells derived from healthy donors. We observed that excessive glucose levels did not affect the percentage of *in vitro* expanded Vδ2 cells in the total CD3$^+$ T cell population, but induced LAG-3 expression (Figure 6G). Nonetheless, switching from normal (NG) to high glucose (HG, 25 or 50 mM) and vice versa could indeed impair or restore expressions of

Figure 3. Transcriptome profiling of γδ T cells in the PBMC of both TB and healthy donors with single-cell RNA sequencing

(A) Schematic overview of the experiment workflow (n = 4 for TB, n = 3 for healthy).

(B) Uniform manifold approximation and projection (UMAP) plot visualization of CD45$^+$ cell clusters from the PBMCs of TB and healthy donors. Immune cell frequency of B, T, NK, and monocyte was also compared between TB patients and healthy controls.

(C) Further extraction of the γδ T cell population was achieved using the TRDC$^+$CD3$^+$ marker, followed by the 2D UMAP projection of the re-clustered γδ T cell population. Relative proportion and distribution of clusters of γδ T cells in TB and healthy donors was also shown.

(D) Heatmap from single-cell analysis with cells grouped into clusters according to top 10 marker genes.

(E) UMAP plots showing representative functional marker genes of each cluster.

(F) Heatmap demonstrating functional pathways enrichments of individual clusters.

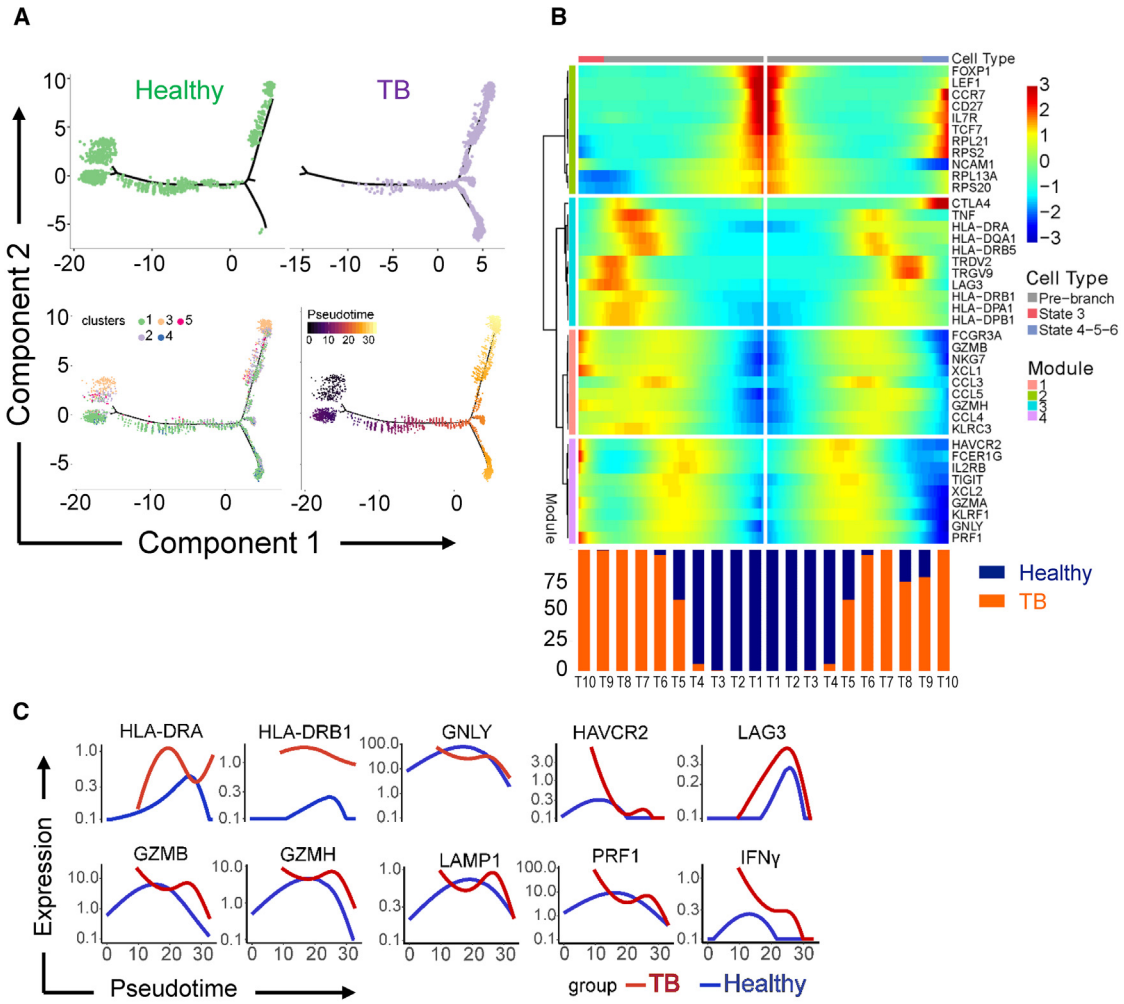

Figure 4. Mapping developmental trajectory by a pseudo-time state transition

(A) Cluster, sample distributions and developmental trajectory of TB or healthy samples using pseudo-time analysis.

(B) Top differentially expressed genes (rows) along pseudo-time were clustered hierarchically and generated four unique gene modules. The top 10 genes in each expression profile are shown (upper panel with rainbow color). The corresponding TB (orange) and healthy (dark blue) sample distribution profile (the lower bar graph) is also overlaid with the gene expression profile to correlate sample distribution.

(C) The pseudo-time trajectory of representative functional genes of healthy or TB samples.

degranulation molecule CD107a (Figure 6H). Intriguingly, the expression of IFN-γ and TNF-α, two important cytokines involved in anti-TB responses, were upregulated in response to excessive glucose. These expression levels could be restored when glucose levels were normalized (Figure 6I). This collectively suggests that high glucose stimulation does not inhibit the secretion of Th1-type cytokines (IFN-γ, TNF-α) by Vδ2 T cells. However, it substantially impairs the degranulation process critical for Vδ2 T-mediated TB-infected cell clearance. Additionally, other phenotypic molecules including CD73, PD1, perforin, and granzyme B, except FasL, did not exhibit significant variations across various glucose concentrations (Figures S4B, S4C). Furthermore, the expression of Ki67, a marker used to assess cell proliferation as it is expressed during the active phases of the cell cycle (G1, S, G2, and mitosis) but absent in resting cells (G0), revealed that high glucose contributed to decreased Ki67 expression (Figure 6J). However, when the culture medium was switched from HG to NG, the expression of Ki67 was restored, suggesting that excess glucose has damaging effects on cell proliferation and such effects are reversible. These findings align well with the cell cycle analysis conducted on γδ T cells of TB patients (Figure 5C). These results suggest a complex regulatory role of glucose in impairing the functions of $V\delta2^+$ T cells.

Hyperglycemia connects with MDR-TB and poor prognosis

The primary challenge in clinically treating active TB patients is the emergence of multidrug-resistant TB (MDR-TB), largely stemming from patients not adhering to the prescribed medication regimen as directed by their physician. Herein, we collected samples to evaluate the functional disparities among $CD8^+$, $V\delta1^+$, and $V\delta2^+$ T cell subsets, with a particular focus on $V\delta2^+$

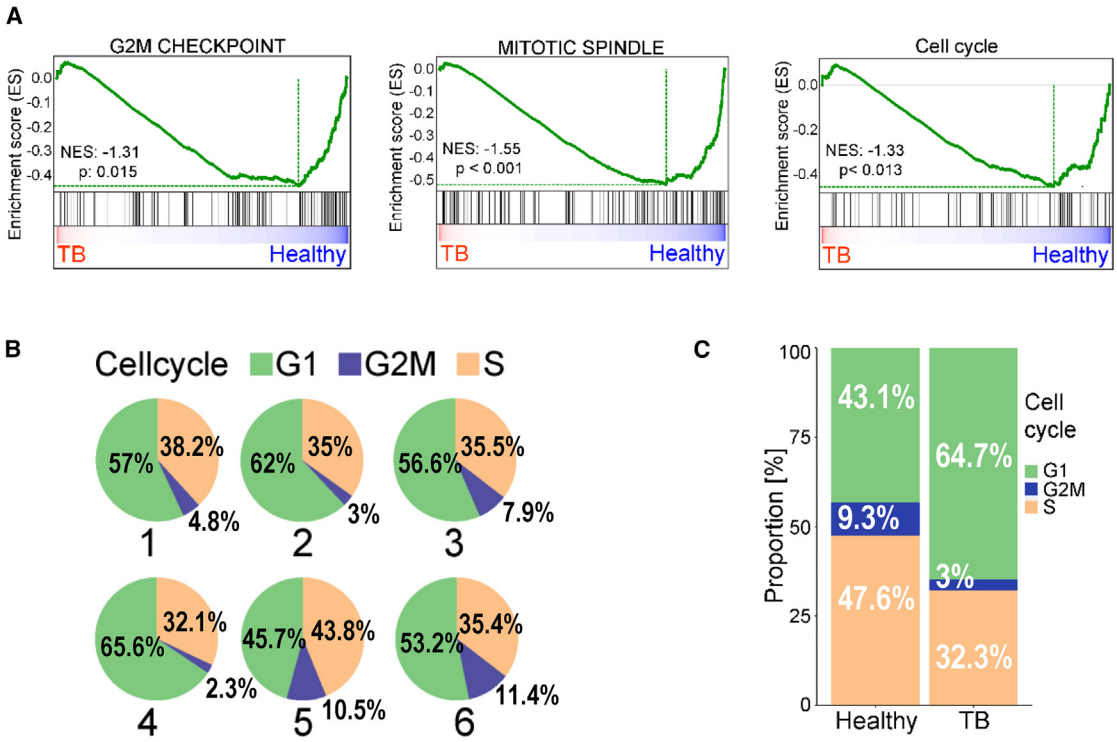

Figure 5. Cell cycle analyses performed using scRNAseq on the PBMCS of TB and healthy donors

(A) GSEA analyses of G2M checkpoint, mitotic spindle, and cell cycle on TB and healthy samples.

(B) Cell cycle phase distribution and respective ratios among six clusters.

(C) Cell cycle phase distribution comparison and respective ratios between TB and healthy samples.

T cells, in both active TB and active MDR-TB patients. We conducted comparisons of T cell ratios, checkpoint molecules, and effector molecules between the two groups (Figures 7A, 7B and S5A). Although no significant differences were found in cell ratios and checkpoint molecules, we observed a considerable decrease in CD107a and IL17 expression, accompanied by an increase in IFNγ protein expression, in Vδ2+ T cells from MDR-TB patients. The downregulation of CD107a and upregulation of IFNγ in MDR-TB patients indicates functional dysregulation within this cohort. IFNγ is a pro-inflammatory Th1 cytokine pivotal in host defense against intracellular pathogens, whereas IL-17 primarily contributes to inflammation and defense against extracellular pathogens. Since TB is an intracellular pathogen, these findings suggest that the anti-TB Th1 cytokine-releasing function of $V\delta2^+$ T cells remains intact in MDR-TB patients. However, the degranulation process necessary for perforin-granzyme-mediated lytic function may be impaired. Similar downregulation of CD107a on $V\delta1^+$ and $CD8^+$ T cells was also observed (Figures S5B, S5C, and S5D). In conclusion, our findings underscore the adverse impact of hyperglycemia on the cytotoxic capabilities of γδ T and $CD8^+$ T cells in TB, consequently heightening the susceptibility to TB progression and the emergence of multidrug resistance.

Hyperglycemia has been established as a factor linked to TB progression to MDR-TB.[27] Therefore, we conducted a comparison of serum glucose levels between patients diagnosed with regular TB and those with MDR-TB (Tables S1 and S2). Our findings reveal that a higher percentage of MDR-TB patients (56.25%) exceeded the normal range of serum glucose (3.89–6.11 nmol/L) compared to regular TB patients (39.58%), suggesting a potential correlation between blood glucose levels and TB progression, as well as drug resistance (Figure 7C). Additionally, we quantified the levels of lactate dehydrogenase (LDH), a key enzyme in the glycolysis pathway (Figure 7D), in TB or MDR-TB patients. LDH catalyzes the conversion of pyruvate to lactate, a process associated with the impairment of T cell effector functions. However, no significant difference in LDH concentration was observed in serum samples from TB and MDR-TB patients. Nevertheless, the MDR-TB cohort exhibited a higher proportion (23.96% vs. 18.75%) of patients exceeding the normal range of LDH concentration compared to the TB cohort (Figure 7E). Furthermore, C-reactive protein (CRP), a critical clinical marker of systemic inflammation and an indicator of immunosuppression, was significantly elevated in both regular active TB and MDR-TB patients. This elevation was noted in 91.67% of TB patients and 95.83% of MDR-TB patients, indicating that CRP levels in both cohorts surpassed the normal range (<6 mg/L in healthy individuals) (Figure 7F). Based on these findings, we speculate that serum glucose levels may play a crucial role in determining the anti-TB functions of Vδ2 T cells.

Additionally, to assess the correlation between hyperglycemia and the clinical outcome of TB patients, we analyzed

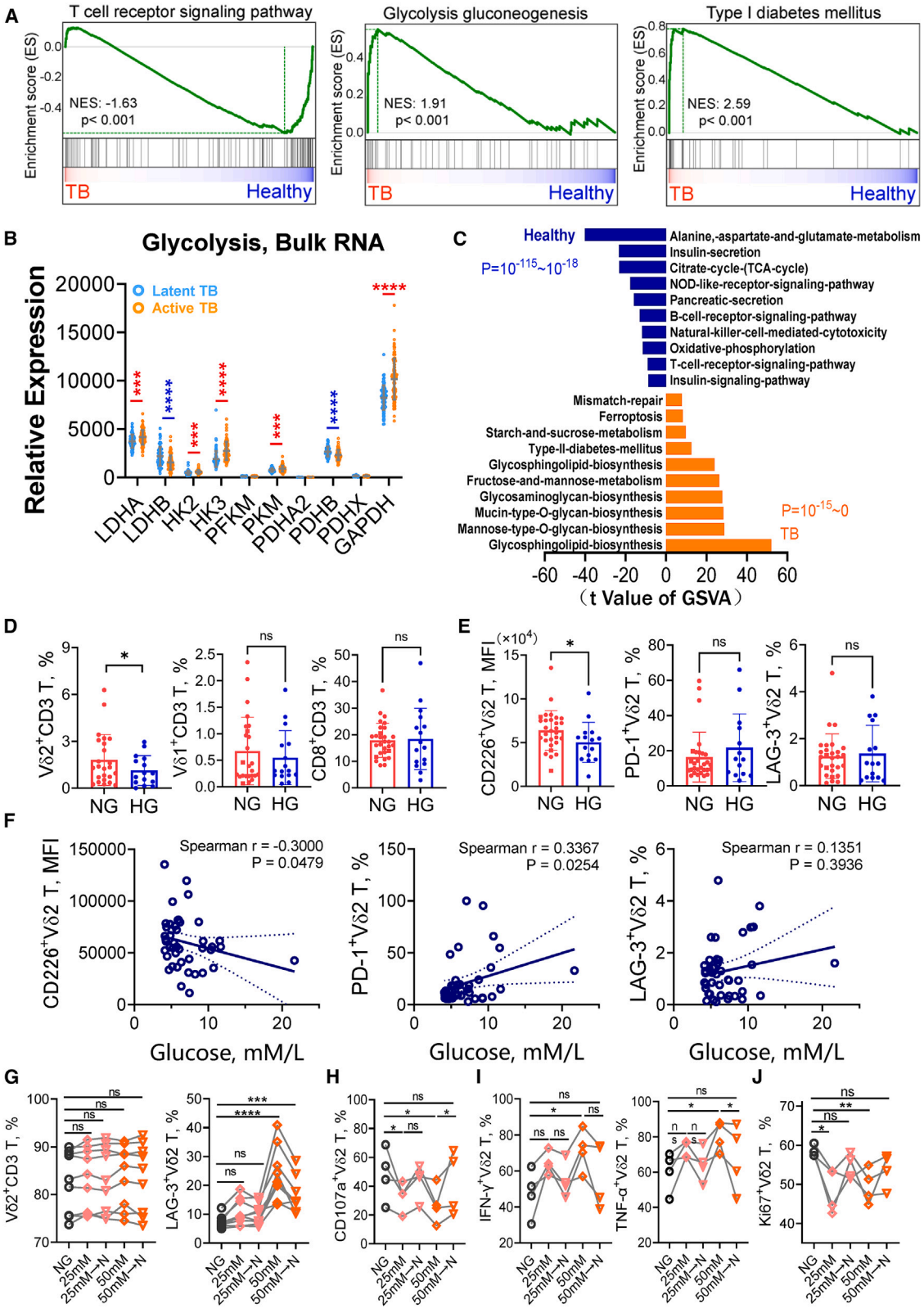

(legend on next page)

sputum smear conversion time and serum glucose levels. Our analysis reveals a positive correlation between the two factors (Figure 7G). Moreover, the clinical data demonstrates a significant prolonged sputum conversion time in TB patients with T2DM (Figure 7H). Notably, 100% of TB alone patients achieved P→N (TB positive to negative) within 70 days, while 30% of TB patients with T2DM remained *M.tb*-positive after 70 days of anti-TB treatment (Figure 7I). Further P→N curve analyses clearly indicated that the 'TB + T2DM' patients have significantly prolonged P→N time than the TB alone patients ($p < 0.0001$) (Figure 7J). In summary, such findings show the detrimental effects of hyperglycemia on the cytotoxic functions of γδ T cells in TB, thereby increasing the risk of TB progression and the development of multi-drug resistance. In summary, these findings emphasize the substantial impact of hyperglycemia, particularly in patients with comorbid T2DM, on sputum smear conversion time and TB clinical outcomes.

DISCUSSION

γδ T cells, particularly Vγ9Vδ2 T cells, play a pivotal role in combating pathogen invasion, serving as the frontline defenders in TB patients. They serve as a vital link between innate and adaptive immunity, recognizing and eliminating pathogen-infected host cells in an MHC-independent manner.[26] Our previous pioneering research introduced allogeneic Vγ9Vδ2 T cells as a clinical intervention for MDR-TB, showing their ability to safely and effectively treat patients, which includes promoting the repair of pulmonary lesions, improving host immunity, and alleviating M. tuberculosis load *in vivo*.[5] However, the observation that only a subset of MDR-TB patients significantly benefited from this treatment prompts scientific inquiry into the fate of allogeneic Vγ9Vδ2 T cells upon administration.

To decipher the underlying mechanism, a comprehensive understanding of the functional characteristics of Vγ9Vδ2 T cells in TB patients is imperative. Based on such context, we started from public databases' mining. We unveil dysregulated immune phenotypes among latent *M.tb*-infected populations, highlighting alterations in checkpoint molecule expression, recognition/activation pathways, and cytokine profiles. Notably, active *M.tb* infection induces more substantial changes in gene expression profiles then latent *M.tb* infection, underscoring the systemic impact of active *M.tb* infection on peripheral immune cell function.

Subsequent examinations demonstrate that active *M.tb* infection markedly diminishes the proportion of Vδ2 T cells within the $CD3^+$ T cell population, resulting in an inversion of the Vδ1/Vδ2 ratio compared to that in healthy individuals. This alteration is presumably induced by the depletion of the $V\delta2^+$ subset triggered by recurrent antigenic stimuli, while the "innate" $V\delta2^+$ population may undergo activation-induced cell death (AICD) owing to the persistent release of phospho-antigens by *M.tb*-infected host cells, such as macrophages. These observations parallel those seen in cancer patients[2,25,26,28] and in sub-healthy population.[29] Our results suggest that the Vδ1/Vδ2 ratio could serve as a potential immune status marker.

Nevertheless, at the functional level, Vδ2 T cells from TB patients exhibited signs of dysfunction, including decreased expression of NKG2D, IFNγ and TNFα. These molecules play crucial roles in immune regulation and clearance of *M.tb*, so their reduced expression may weaken the patient's immune response. However, the elevated levels of CD226 and CD107a suggest that Vδ2 T cells still retain some cytotoxic potential, which may be related to the delicate balance between pro-inflammatory IL-17 and immunosuppressive TGFβ. Although we did not observe statistical differences in the expression of PD-1, LAG-3, IFNγ, TNFα and CD107a between normal (NG) and hyperglycemia (HG) TB patients, *in vitro* experiments indicate that high glucose levels alone may impair the anti-TB functions of Vδ2 T cells. This finding suggests that hyperglycemia may further exacerbate the immune deficiency in TB patients by affecting the function of Vδ2 T cells.

While extensive research has focused on Vδ2 T cells in TB, particularly by the Zheng W Chen group,[4,30–33] transcriptomic profiling of single γδ T cells in TB patients remains unexplored. scRNA-seq revealed an activated yet functionally impaired state in γδ T cells, characterized by compromised proliferation and upregulated inhibitory checkpoint genes suggestive of cellular exhaustion induced by the long-term stimulation of *M.tb* infection.

Moreover, the emergence of MDR-TB presents a formidable clinical challenge, potentially exacerbated by factors such as non-compliance with treatment regimens and the physiological microenvironment. Our investigation identified elevated serum glucose and CRP levels in MDR-TB patients, hinting at a possible association with hyperglycemia. Given the well-established link between TB and hyperglycemia/diabetes, our study delves into the immune responses, particularly on γδ T cells, revealing reversible functional impairments induced by hyperglycemia.

Figure 6. Clinical immune phenotyping and *in vitro* validation of the role of high glucose levels in undermining the immune functions of Vδ2 T cells

(A) GSEA analyses of TCR signaling, glycolysis-gluconeogenesis, and type 1 diabetes of γδ T cells in TB and healthy samples using the scRNA-seq data.

(B) Gene expression of key glycolytic enzymes derived from the PBMCs of active ($n = 97$) and latent ($n = 83$) TB samples using bulk RNA-seq data from the GEO database (GSE37250). Red *, upregulation in active TB; blue *, downregulation in active TB.

(C) GVSA analyses of glucose metabolism related pathways of γδ T cells on TB and healthy samples using the scRNA-seq data.

(D and E) $V\delta2^+$, $V\delta1^+$, and $CD8^+$ T cell ratios, as well as CD226(DNAM-1), PD-1, and LAG3 expressions on Vδ2 T cells in TB patients with normal (NG) or high serum glucose levels (hyperglycemia, HG). Each dot on the graphs represents an individual patient. According to the clinical guideline in China, NG: 3.89 to 6.11 mmol/L, HG: 7.0 mmol/L or above.

(F) Correlations between the expression of CD226, PD-1, and LAG3 on peripheral Vδ2 T cells and serum glucose levels in TB patients.

(G–J) Phenotype evaluations, including Vδ2 ratio in CD3 T, and expression of LAG3, CD107a, IFNγ, TNFα, and Ki67 of $V\delta2^+$ T cells under NG, HG (25 and 50 mM), or HG→NG using *in vitro* expanded $V\delta2^+$ derived from healthy donors. Each connected curve on the graphs represents cell samples obtained from individual donors. Quantitative data are shown as the mean ± SD. $^*p < 0.05$, $^{**}p < 0.01$, $^{***}p < 0.001$, $^{****}p < 0.0001$; ns, not significant. Data are represented as mean ± SD.

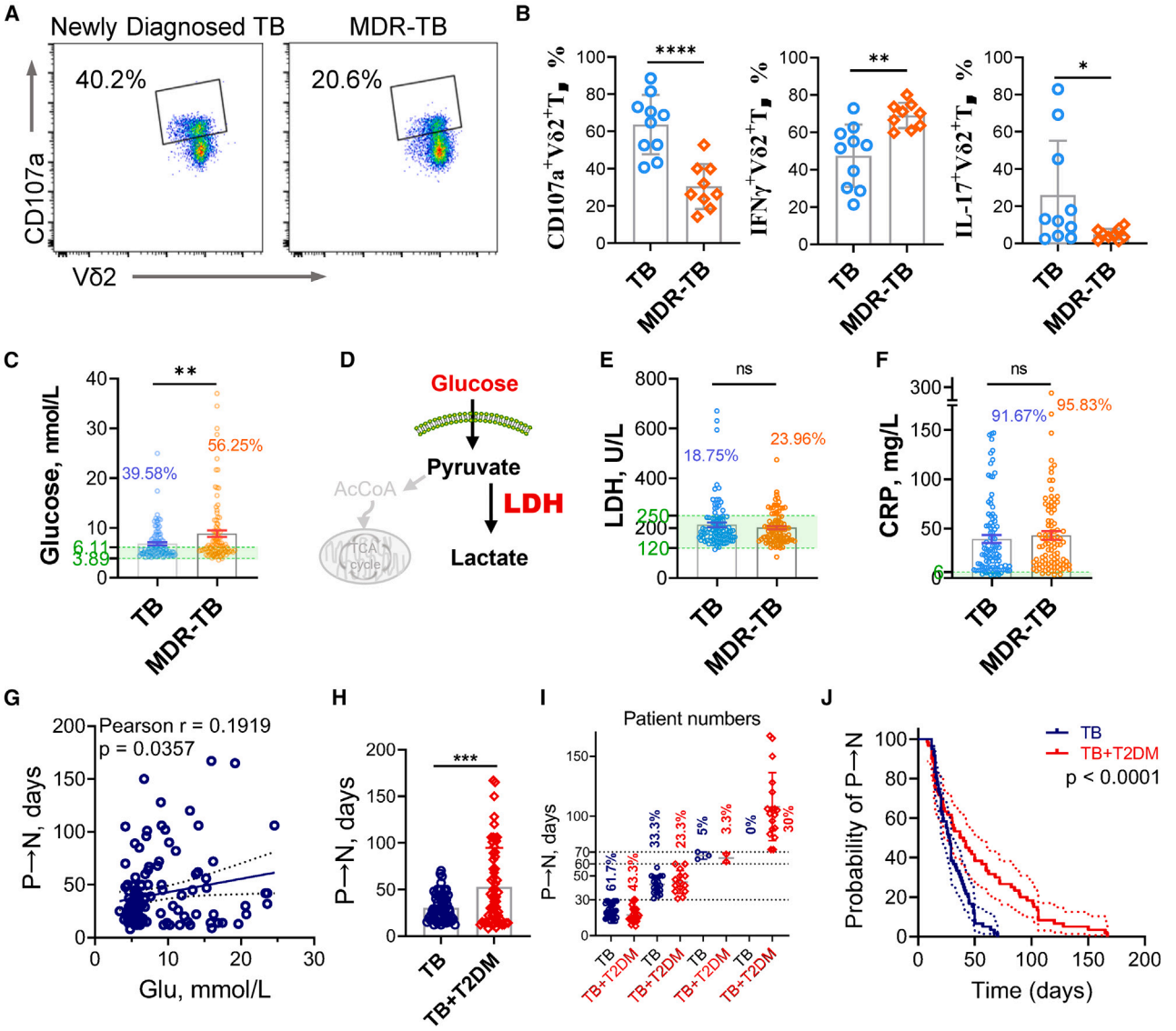

Figure 7. Immune phenotyping of Vδ2 T cells in regular TB and MDR-TB patients, as well as analyses of clinical correlation between glucose and TB prognosis

(A) Representative flow plots of CD107a$^+$ Vδ2 T cells in TB and MDR-TB patients.

(B) Expressions of CD107a, IFNγ, and IL17 in Vδ2 T cells in TB and MDR-TB patients. Patient numbers for a-b, regular active TB: $n = 10$, MDR-TB: $n = 9$.

(C) Clinical statistics of serum glucose level in TB and MDR-TB patients. The scale range highlighted by green dashed lines shows the normal range of serum glucose in healthy populations (3.89–6.11 nmol/L). The serum glucose level exceeds the normal range in 39.58% of TB patients and 56.25% of MDR-TB patients.

(D) Sketch of glucose metabolism.

(E and F) Measurements on the serum levels of LDH and CRP, respectively ($n = 96$ for each group). The percentage marked in the graphs represents the percentage of TB/MDR-TB patients with elevated levels of LDH or CRP. For example, 18.75% of TB patients have serum LDH outside the normal range (120–250 U/L), while 23.96% of MDR-TB patients has serum LDH outside the normal range (e). The normal range for serum CRP is typically less than 6 mg/L (f).

(G) Retrospective clinical data analyses on the sputum smear transition time from TB positive to negative (P→N) and its positive correlation with serum glucose level.

(H and I) Retrospective clinical data analyses on the sputum smear transition time (P→N) comparison between TB patients with or without T2DM. (h): Group overview of P→N between TB and 'TB + T2DM'; (i): Detailed analyses. Within 30 days, the percentage of P→N of 'TB + T2DM' group (43.3%) is apparently lower than that of TB group (61.7%). Within 60 days, the percentage of P→N of 'TB + T2DM' group (66.6%) is apparently lower than that of TB group (95%) as well. 100% of TB patients achieved P→N within 70 days. There are 30% 'TB + T2DM' patients are still *M.tb*-positive after 70 days of anti-TB treatment.

(J) Probability curve of P→N of two groups TB and 'TB + T2DM', showing significantly prolonged P→N time of the group 'TB + T2DM' ($p < 0.0001$). ($n = 60$ for each group). Data are represented as mean ± SD, or SEM (c, e, f). *$p < 0.05$, **$p < 0.01$, ***$p < 0.001$, ****$p < 0.0001$; ns, not significant.

Such observation also implies that excessive serum glucose may contribute to the dysfunctions of Vδ2 T cells, which could be partially supported by the positive correlations between hyperglycemia and the depressed Vδ2 T cell functions, as well as the prolonged time for *M.tb* conversion to negative status. However, this hypothesis requires further experimental evidence to establish a definitive cause-and-effect relationship.

We provide insights into disease progression by examining distinct response patterns in $V\delta1^+$ and $V\delta2^+$ T cells in the presence of hyperglycemia. Further research on molecular mechanism such as exploring posttranslational glycosylation and epigenetic modifications, can uncover the interplay between γδ T cell subsets and TB pathogenesis. Managing TB and hyperglycemia is crucial, as hyperglycemia negatively affects γδ T cell functions. This heightens risk of MDR-TB in hyperglycemic TB patients, underscoring the urgent need for integrated management strategies. Screening for TB in individuals with diabetes, along with effective hyperglycemia management, are essential for better treatment outcomes. Integrated approaches involving TB control programs and collaboration between healthcare providers are necessary for improved management in individuals with both conditions.

Limitations of this study

Despite above insights, our study has several limitations warranting future exploration. Notably, the functional transformation of γδ T cells within the pulmonary microenvironment remains unexplored, necessitating analysis of alveolar lavage fluid samples. Additionally, leveraging matched samples from different TB stages and drug resistance profiles will elucidate functional signatures of γδ T cells throughout the progression of the disease. Furthermore, while our findings suggest a link between hyperglycemia and Vδ2 T cell dysfunction, mechanistic validation is warranted to establish causality. Additionally, the scRNA-seq data reveal that NK cells, another cytotoxic population, are expanded in TB patients compared to healthy individuals. Investigating the underlying cytotoxicity mechanisms of NK cells alongside γδ T cells in TB could further enhance our understanding of the immune responses in these patients. In conclusion, addressing these limitations will advance our understanding of γδ T cell regulation in TB and inform alternative treatment strategies, underscoring the importance of integrated approaches for TB and hyperglycemia management.

RESOURCE AVAILABILITY

Lead contact

Additional information for resources should be directed to the lead contact, Yi Hu (yihu2020@jnu.edu.cn).

Materials availability

This work did not generate new unique reagents.

Data and code availability

- Data: The scRNA-seq data of TB patients are available in Genome Sequence Archive (HRA000910, https://ngdc.cncb.ac.cn/gsa-human/browse/HRA000910; HRA000363, https://ngdc.cncb.ac.cn/gsa-human/browse/HRA000363).
- Code: This work does not generate unique code.
- Other items: N/A.

ACKNOWLEDGMENTS

We thank Ms. Xiaoying Lu from the OE Biotech Co., Ltd for assisting with analysis of the single cell data.

Funding.

This work was supported by the "DengfengPlan" High-level Hospital Construction Opening Project of the Foshan Fourth People's Hospital (No. FSSYKF-2020016). Meanwhile, Y.H. is supported by the National Natural Science Foundation of China (82002787); Y.Z.W. is supported by the National Natural Science Foundation of China (32270950) and partially by the Key Program of the National Natural Science Foundation of China (32030036).

AUTHOR CONTRIBUTIONS

Work supervision and protocol design: Y.H. and Y.Z.W. Experiments: Y.H., J.L., and Y.Y.J. Clinical sample and data collection: M.Y.L., Y.Q.S., X.Z.W., Q.L.H., and J.L. Data analysis and discussion: Y.H., Y.Z.W., M.J.H., Y.J.L., C.X., G.H.Z., and Y.C. Manuscript writing and revision: Y.H. and Y.Z.W. All authors approved the final version of manuscript.

DECLARATION OF INTERESTS

The authors declare no competing interests.

STAR★METHODS

Detailed methods are provided in the online version of this paper and include the following:

- KEY RESOURCES TABLE
- EXPERIMENTAL MODEL AND STUDY PARTICIPANT DETAILS
- METHOD DETAILS
  - Selective expansion of Vγ9Vδ2 T cells from PBMCs and subsequent glucose treatment
  - Single-cell RNA sequencing of PBMCs from TB patients
  - Utilization of online database of bulk-RNA transcriptome
  - Phenotypic markers detection by flow cytometry
- QUANTIFICATION AND STATISTICAL ANALYSIS

SUPPLEMENTAL INFORMATION

Supplemental information can be found online at https://doi.org/10.1016/j.isci.2024.111692.

Received: August 25, 2024
Revised: October 25, 2024
Accepted: December 23, 2024
Published: December 26, 2024

REFERENCES

1. Pai, M. (2020). Tuberculosis: the story after the Primer. Nat. Rev. Dis. Prim. *6*, 29. https://doi.org/10.1038/s41572-020-0161-5.
2. Dheda, K., and Lange, C. (2022). A revolution in the management of multidrug-resistant tuberculosis. Lancet *400*, 1823–1825. https://doi.org/10.1016/S0140-6736(22)02161-4.
3. Chandra, P., Grigsby, S.J., and Philips, J.A. (2022). Immune evasion and provocation by Mycobacterium tuberculosis. Nat. Rev. Microbiol. *20*, 750–766. https://doi.org/10.1038/s41579-022-00763-4.
4. Shen, L., Frencher, J., Huang, D., Wang, W., Yang, E., Chen, C.Y., Zhang, Z., Wang, R., Qaqish, A., Larsen, M.H., et al. (2019). Immunization of Vgamma2Vdelta2 T cells programs sustained effector memory responses that control tuberculosis in nonhuman primates. Proc. Natl. Acad. Sci. USA *116*, 6371–6378. https://doi.org/10.1073/pnas.1811380116.
5. Liang, J., Fu, L., Li, M., Chen, Y., Wang, Y., Lin, Y., Zhang, H., Xu, Y., Qin, L., Liu, J., et al. (2021). Allogeneic Vgamma9Vdelta2 T-Cell Therapy

Promotes Pulmonary Lesion Repair: An Open-Label, Single-Arm Pilot Study in Patients With Multidrug-Resistant Tuberculosis. Front. Immunol. *12*, 756495. https://doi.org/10.3389/fimmu.2021.756495.

6. Nielsen, M.M., Witherden, D.A., and Havran, W.L. (2017). gammadelta T cells in homeostasis and host defence of epithelial barrier tissues. Nat. Rev. Immunol. *17*, 733–745. https://doi.org/10.1038/nri.2017.101.
7. Silva-Santos, B., and Strid, J. (2017). gammadelta T cells get adaptive. Nat. Immunol. *18*, 370–372. https://doi.org/10.1038/ni.3705.
8. Brandes, M., Willimann, K., and Moser, B. (2005). Professional antigen-presentation function by human gammadelta T Cells. Science *309*, 264–268. https://doi.org/10.1126/science.1110267.
9. Brandes, M., Willimann, K., Bioley, G., Lévy, N., Eberl, M., Luo, M., Tampé, R., Lévy, F., Romero, P., and Moser, B. (2009). Cross-presenting human gammadelta T cells induce robust CD8+ alphabeta T cell responses. Proc. Natl. Acad. Sci. USA *106*, 2307–2312. https://doi.org/10.1073/pnas.0810059106.
10. Caccamo, N., Battistini, L., Bonneville, M., Poccia, F., Fournié, J.J., Meraviglia, S., Borsellino, G., Kroczek, R.A., La Mendola, C., Scotet, E., et al. (2006). CXCR5 identifies a subset of Vgamma9Vdelta2 T cells which secrete IL-4 and IL-10 and help B cells for antibody production. J. Immunol. *177*, 5290–5295. https://doi.org/10.4049/jimmunol.177.8.5290.
11. Caccamo, N., Sireci, G., Meraviglia, S., Dieli, F., Ivanyi, J., and Salerno, A. (2006). gammadelta T cells condition dendritic cells in vivo for priming pulmonary CD8 T cell responses against Mycobacterium tuberculosis. Eur. J. Immunol. *36*, 2681–2690. https://doi.org/10.1002/eji.200636220.
12. Martino, A., and Poccia, F. (2007). Gamma delta T cells and dendritic cells: close partners and biological adjuvants for new therapies. Curr. Mol. Med. *7*, 658–673. https://doi.org/10.2174/156652407782564345.
13. Spencer, C.T., Abate, G., Sakala, I.G., Xia, M., Truscott, S.M., Eickhoff, C.S., Linn, R., Blazevic, A., Metkar, S.S., Peng, G., et al. (2013). Granzyme A produced by gamma(9)delta(2) T cells induces human macrophages to inhibit growth of an intracellular pathogen. PLoS Pathog. *9*, e1003119. https://doi.org/10.1371/journal.ppat.1003119.
14. Willcox, B.E., and Willcox, C.R. (2019). gammadelta TCR ligands: the quest to solve a 500-million-year-old mystery. Nat. Immunol. *20*, 121–128. https://doi.org/10.1038/s41590-018-0304-y.
15. Silva-Santos, B., Mensurado, S., and Coffelt, S.B. (2019). gammadelta T cells: pleiotropic immune effectors with therapeutic potential in cancer. Nat. Rev. Cancer *19*, 392–404. https://doi.org/10.1038/s41568-019-0153-5.
16. Vantourout, P., and Hayday, A. (2013). Six-of-the-best: unique contributions of gammadelta T cells to immunology. Nat. Rev. Immunol. *13*, 88–100. https://doi.org/10.1038/nri3384.
17. Davey, M.S., Willcox, C.R., Hunter, S., Kasatskaya, S.A., Remmerswaal, E.B.M., Salim, M., Mohammed, F., Bemelman, F.J., Chudakov, D.M., Oo, Y.H., and Willcox, B.E. (2018). The human Vdelta2(+) T-cell compartment comprises distinct innate-like Vgamma9(+) and adaptive Vgamma9(-) subsets. Nat. Commun. *9*, 1760. https://doi.org/10.1038/s41467-018-04076-0.
18. Mensurado, S., Blanco-Domínguez, R., and Silva-Santos, B. (2023). The emerging roles of γδ T cells in cancer immunotherapy. Nat. Rev. Clin. Oncol. *20*, 178–191. https://doi.org/10.1038/s41571-022-00722-1.
19. Eckold, C., Kumar, V., Weiner, J., Alisjahbana, B., Riza, A.L., Ronacher, K., Coronel, J., Kerry-Barnard, S., Malherbe, S.T., Kleynhans, L., et al. (2021). Impact of Intermediate Hyperglycemia and Diabetes on Immune Dysfunction in Tuberculosis. Clin. Infect. Dis. *72*, 69–78. https://doi.org/10.1093/cid/ciaa751.
20. Restrepo, B.I., Fisher-Hoch, S.P., Pino, P.A., Salinas, A., Rahbar, M.H., Mora, F., Cortes-Penfield, N., and McCormick, J.B. (2008). Tuberculosis in poorly controlled type 2 diabetes: altered cytokine expression in peripheral white blood cells. Clin. Infect. Dis. *47*, 634–641. https://doi.org/10.1086/590565.
21. Riza, A.L., Pearson, F., Ugarte-Gil, C., Alisjahbana, B., van de Vijver, S., Panduru, N.M., Hill, P.C., Ruslami, R., Moore, D., Aarnoutse, R., et al. (2014). Clinical management of concurrent diabetes and tuberculosis and the implications for patient services. Lancet Diabetes Endocrinol. *2*, 740–753. https://doi.org/10.1016/S2213-8587(14)70110-X.
22. Gautam, S., Shrestha, N., Mahato, S., Nguyen, T.P.A., Mishra, S.R., and Berg-Beckhoff, G. (2021). Diabetes among tuberculosis patients and its impact on tuberculosis treatment in South Asia: a systematic review and meta-analysis. Sci. Rep. *11*, 2113. https://doi.org/10.1038/s41598-021-81057-2.
23. Zhang, D., Jin, W., Wu, R., Li, J., Park, S.A., Tu, E., Zanvit, P., Xu, J., Liu, O., Cain, A., and Chen, W. (2019). High Glucose Intake Exacerbates Autoimmunity through Reactive-Oxygen-Species-Mediated TGF-beta Cytokine Activation. Immunity *51*, 671–681e5. https://doi.org/10.1016/j.immuni.2019.08.001.
24. Mu, X., Xiang, Z., Xu, Y., He, J., Lu, J., Chen, Y., Wang, X., Tu, C.R., Zhang, Y., Zhang, W., et al. (2022). Glucose metabolism controls human gammadelta T-cell-mediated tumor immunosurveillance in diabetes. Cell. Mol. Immunol. *19*, 944–956. https://doi.org/10.1038/s41423-022-00894-x.
25. Hu, Y., Chen, D., Hong, M., Liu, J., Li, Y., Hao, J., Lu, L., Yin, Z., and Wu, Y. (2022). Apoptosis, Pyroptosis, and Ferroptosis Conspiringly Induce Immunosuppressive Hepatocellular Carcinoma Microenvironment and gammadelta T-Cell Imbalance. Front. Immunol. *13*, 845974. https://doi.org/10.3389/fimmu.2022.845974.
26. Hu, Y., Hu, Q., Li, Y., Lu, L., Xiang, Z., Yin, Z., Kabelitz, D., and Wu, Y. (2023). γδ T cells: origin and fate, subsets, diseases and immunotherapy. Signal Transduct. Targeted Ther. *8*, 434. https://doi.org/10.1038/s41392-023-01653-8.
27. Xu, G., Hu, X., Lian, Y., and Li, X. (2023). Diabetes mellitus affects the treatment outcomes of drug-resistant tuberculosis: a systematic review and meta-analysis. BMC Infect. Dis. *23*, 813. https://doi.org/10.1186/s12879-023-08765-0.
28. He, W., Hu, Y., Chen, D., Li, Y., Ye, D., Zhao, Q., Lin, L., Shi, X., Lu, L., Yin, Z., et al. (2022). Hepatocellular carcinoma-infiltrating gammadelta T cells are functionally defected and allogenic Vdelta2(+) gammadelta T cell can be a promising complement. Clin. Transl. Med. *12*, e800. https://doi.org/10.1002/ctm2.800.
29. Jia, Z., Ren, Z., Ye, D., Li, J., Xu, Y., Liu, H., Meng, Z., Yang, C., Chen, X., Mao, X., et al. (2023). Immune-Ageing Evaluation of Peripheral T and NK Lymphocyte Subsets in Chinese Healthy Adults. Phenomics *3*, 360–374. https://doi.org/10.1007/s43657-023-00106-0.
30. Chen, Z.W. (2013). Multifunctional immune responses of HMBPP-specific Vgamma2Vdelta2 T cells in M. tuberculosis and other infections. Cell. Mol. Immunol. *10*, 58–64. https://doi.org/10.1038/cmi.2012.46.
31. Chen, Z.W. (2016). Protective immune responses of major Vgamma2Vdelta2 T-cell subset in M. tuberculosis infection. Curr. Opin. Immunol. *42*, 105–112. https://doi.org/10.1016/j.coi.2016.06.005.
32. Shen, Y., Zhou, D., Qiu, L., Lai, X., Simon, M., Shen, L., Kou, Z., Wang, Q., Jiang, L., Estep, J., et al. (2002). Adaptive immune response of Vgamma2Vdelta2+ T cells during mycobacterial infections. Science *295*, 2255–2258. https://doi.org/10.1126/science.1068819.
33. Qaqish, A., Huang, D., Chen, C.Y., Zhang, Z., Wang, R., Li, S., Yang, E., Lu, Y., Larsen, M.H., Jacobs, W.R., Jr., et al. (2017). Adoptive Transfer of Phosphoantigen-Specific gammadelta T Cell Subset Attenuates Mycobacterium tuberculosis Infection in Nonhuman Primates. J. Immunol. *198*, 4753–4763. https://doi.org/10.4049/jimmunol.1602019.

STAR★METHODS

KEY RESOURCES TABLE

REAGENT or RESOURCE	SOURCE	IDENTIFIER
Antibodies		
Mouse anti-human monoclonal CD3	Biolegend	Cat#300306; RRID: AB_314042
Mouse anti-human monoclonal TCRVδ2	Biolegend	Cat#331408; RRID: AB_1089232
Mouse anti-human monoclonal TCRVδ1	Miltenyi	Cat#130118968; RRID: AB_2733451
Mouse anti-human monoclonal CD8	BD Biosciences	Cat#563256; RRID: AB_2738101
Mouse anti-human monoclonal CD73	Biolegend	Cat#344024; RRID: AB_2650974
Mouse anti-human monoclonal PD1	BD Biosciences	Cat#564323; RRID: AB_2738745
Mouse anti-human monoclonal LAG3	Biolegend	Cat#369316; RRID: AB_2632951
Mouse anti-human monoclonal CD226	Biolegend	Cat#338322; RRID: AB_2721560
Mouse anti-human monoclonal NKG2D	Biolegend	Cat#320834; RRID: AB_2734297
Mouse anti-human monoclonal CD107a	Biolegend	Cat#328640; RRID: AB_2565840
Mouse anti-human monoclonal IFNγ	Biolegend	Cat#502520; RRID: AB_528921
Mouse anti-human monoclonal IL-17A	BD Biosciences	Cat#560436; RRID: AB_1645514
Mouse anti-human monoclonal TNFα	Biolegend	Cat#502936; RRID: AB_2563884
Mouse anti-human monoclonal TGFβ	BD Biosciences	Cat#562962; RRID: AB_2737919
Mouse IgG1, κ Isotype Ctrl Antibody	Biolegend	Cat#400196; RRID: N/A
Mouse IgG1, κ Isotype Ctrl Antibody	Biolegend	Cat#400170; RRID: N/A
Mouse IgG1, κ Isotype Ctrl Antibody	Biolegend	Cat#400164; RRID: N/A
Biological samples		
Blood of healthy adult and TB patient	The Forth People's Hospital of Foshan	N/A
Chemicals, peptides, and recombinant proteins		
Recombinant human interleukin-2	Beijing Four Rings Bio-Pharm Co.	Cat#S20040018
Zoledronate	Sigma-Aldrich	Cat#SML0223
Vitamin C	Sigma-Aldrich	Cat#A4403
Glucose	Sigma-Aldrich	Cat#G7021
Deposited data		
scRNA-seq data of TB patients	Genome Sequence Archive (https://ngdc.cncb.ac.cn/gsa-human/browse/HRA000910; https://ngdc.cncb.ac.cn/gsa-human/browse/HRA000363)	HRA000910; HRA000363.
Software and algorithms		
GraphPad Prism http://www.graphpad.com/	GraphPad	RRID:SCR_002798
FlowJo	BD Life Sciences	FlowJo™ v10.8
R studio	POSIT	RStudio.v4.1
Other		
RPMI-1640 medium	Gibco	Cat#C11875500BT
Fetal bovine serum (FBS)	Sigma- Aldrich	Cat#F8318

EXPERIMENTAL MODEL AND STUDY PARTICIPANT DETAILS

This study followed ethical principles of the Declaration of Helsinki and obtained full approval from the ethical committee of The Forth People's Hospital of Foshan. Prior to blood collection, all participants provided written informed consent. Blood samples were collected from patients at the Forth People's Hospital of Foshan in China. To ensure patient privacy, all sensitive information was removed. Fasting Blood Glucose (FBG) levels, LDH activity, and CRP levels were obtained from regular clinical lab screenings.

CellPress
OPEN ACCESS

Detailed Glucose, LDH, and CRP levels of ninety-six newly diagnosed TB and ninety-six MDR-TB patients were included in Table S2. The clinical diagnosis of new tuberculosis (TB) patients is primarily based on the initial detection of *Mycobacterium tuberculosis* in sputum from individuals who have not previously received TB treatment. For multidrug-resistant TB (MDR-TB), the clinical critia require evidence of no response to at least two key mediciations, isoniazid and rifampicin. Detailed clinical information for TB patients with or without type 2 diabetes (T2D) is provided in Table S3. The classification of TB patients with or without T2D is primarily based on Fasting Blood Glucose (FBG) levels at the time of initial TB diagnosis, with patients having an FBG level greater than 7.0 mmol/L categorized as TB + T2D. Then, sixty TB patients and sixty TB + T2D patients were included in the data collection. As for TB treament, the 4-drug "HREZ" fixed-dose combination (FDC), consisting of isoniazid (H), rifampicin (R), ethambutol (E), and pyrazinamide (Z), was adopted clinically.

METHOD DETAILS

Selective expansion of Vγ9Vδ2 T cells from PBMCs and subsequent glucose treatment

PBMCs isolated from healthy donors were cultured by following the standard Ficoll-Paque density gradient protocol. Then, isolated PBMCs were cultured in Roswell Park Memorial Institute (RPMI)-1640 medium supplemented with 10% fetal bovine serum, recombinant human interleukin-2 (100 IU/mL, Beijing Four Rings Bio-Pharm Co.), zoledronate (50 μM, Sigma), and vitamin C (800 IU/mL, Sigma). On the third day, the PBMCs were treated with normal glucose (11.1 mM, glucose concentration in regular RPMI1640 culture medium) (NG-Vγ9Vδ2 T cells) or high glucose (25 or 50 mM) (HG-Vγ9Vδ2 T cells) to simulate hyperglycemia *in vitro* for 8 days. For HG→NG-Vγ9Vδ2 T cells, they were cultured with normal glucose (11.1 mM, NG) for an additional 16 h (25 or 50 mM→11.1 mM) before subsequent detection.

Single-cell RNA sequencing of PBMCs from TB patients

PBMCs obtained from four TB patients were subjected to single-cell sequencing using the 10× Genomics platform, and the raw data are available in Genome Sequence Archive (HRA000910, https://ngdc.cncb.ac.cn/gsa-human/browse/HRA000910; HRA000363, https://ngdc.cncb.ac.cn/gsa-human/browse/HRA000363). Adanced analyses is briefly introduced as the followings: (1) Developmental pseudotime was determined using the Monocle2 package (v2.9.0). (2) For Gene Set Variation Analysis (GVSA), we utilized the GSEABase package (version 1.44.0) to load the gene set file. (3) Cell cycle phase prediction was conducted using the CellCycleScoring function in Seurat. For comparison, control scRNA data of PBMCs from healthy donors were downloaded from the official website of 10x Genomics (https://www.10xgenomics.com/). Top50 markers for clusters '1–6' are included in the Table S1.

Utilization of online database of bulk-RNA transcriptome

To explore functional differences in TB patients and healthy controls or latent *M.tb* infected populations at the macro level, bulk-RNA transcriptome data (GSE19444 and GSE37250) from the Gene Expression Omnibus (GEO) database were extracted and analyzed.

Phenotypic markers detection by flow cytometry

Cell surface and intracellular markers were stained with mouse anti-human monoclonal antibodies, including anti-CD3 (300306, Biolegend), anti-TCR Vδ2 (331408, Biolegend), anti-TCR Vδ1 (130-118-968, Miltenyi), anti-CD8 (563256, BD Biosciences), anti-CD73 (344024, Biolegend), anti-PD-1 (564323, BD Biosciences), anti-LAG-3 (369316, Biolegend), anti-CD226 (338322, Biolegend), anti-NKG2D (320834, Biolegend), anti-CD107a (328640, Biolegend), anti-IFN-γ (502520, Biolegend), anti-IL-17A (560436, BD Biosciences), anti-TNF-α (502936, Biolegend), anti-TGF-β (562962, BD Biosciences), Mouse IgG1 (κ Isotype Ctrl Antibody, 400196, Biolegend), Mouse IgG1 (κ Isotype Ctrl Antibody, 400170, Biolegend), Mouse IgG1 (κ Isotype Ctrl Antibody, 400164, Biolegend). The prepared samples were measured by Cytek Aurora spectral flow cytometry, with 14 antibodies divided into two panels: one for surface molecules and another for intracellular molecules. To facilitate reproducibility, we included appropriate controls, such as isotype control and fluorescence minus one (FMO) control, to account for non-specific staining and background fluorescence. Regarding the gating and analysis strategy, lymphocytes were first identified based on their FSC-A/SSC-A profiles. To ensure that only single cells were included, doublets and cell aggregates were excluded using FSC-A/FSC-H plots. We identified specific cell subsets, including $CD8^+$ T cells, $V\delta2^+$ γδ T cells, and $V\delta1^+$ γδ T cells, using appropriate markers such as CD8, Vδ2, and Vδ1. For mean fluorescence intensity (MFI) measurement and data quality control, we employed several measures to ensure the reliability of the MFI data. First, we maintained consistent gain and voltage settings throughout all experiments to minimize variability between runs. Second, we reported relative MFI values by normalizing against the control group to account for technical variability. Finally, to enhance reproducibility, we performed repeated experiments and reported the average MFI values to reduce the impact of random variation. Then, the data were analyzed using FlowJo.

QUANTIFICATION AND STATISTICAL ANALYSIS

Statistical analysis was performed using GraphPad Prism software. Data were presented as mean ± standard deviation (SD) or standard error of the mean (SEM). Paired or unpaired Student's t-tests were used to assess statistical significance, unless otherwise indicated. A p-value of <0.05 was considered significant. *$p < 0.05$, **$p < 0.01$, ***$p < 0.001$, ****$p < 0.0001$; unmarked or ns, represents no statistical significance.